

Pyridylenevinylene based Cu²⁺-Specific, Injectable Metallo(hydro)gel: Thixotropy and Nanoscale Metal-Organic Particles

Subham Bhattacharjee,^a and Santanu Bhattacharya^{*a, b}

^aDepartment of Organic Chemistry, Indian Institute of Science, Bangalore, India. Fax: +91-80-23600529; Tel: +91-80-22932664; E-mail: sb@orgchem.iisc.ernet.in

^bJawaharlal Nehru Centre for Advanced Scientific Research, Bangalore, India.

Table of contents:

1. Physical Measurements and Instrumentation.
2. Synthesis.
3. Figure S1: FT-IR spectra of ligand **1** and **1**/Cu²⁺ complex and ESI-MS of **1**/Cu²⁺ complex.
4. Figure S2: Titration of ligand **1** with increasing amount of Cu²⁺ in water under UV-Vis spectroscopy ([**1**] = 25 μM) and determination of binding constant of the **1**/Cu²⁺ complex; UV-Vis spectroscopy of the solution of **1**/Cu²⁺ in various molar ratios at a fixed total concentration of 50 μM and Job's plot of **1** with Cu²⁺ in water; Digital image of the metallo(ge)l of **1** under illumination at 365 nm; Titration of the solution of the ligand **1** (25 μM) in water with increasing proportion of Cu²⁺.
- 5 Figure S3: Concentration dependent emission spectra of the metallo(ge)l and the corresponding photographs of the solutions under UV-light (365 nm) respectively.
6. Figure S4: Demonstration of the gradual abolition of the metallo(ge)l of **1**, when few drops of concentrated NH₄OH were added to the top of the preformed gel.
7. Figure S5: SEM ([**1**] = 0.3 mM) images of the diluted solution of the metallo(ge)l of **1** at different position and magnifications respectively. SEM ([**1**] = 8 mM) image of the metallo(ge)l of **1** obtain after drop-casting of the metallo(ge)l directly onto the silicon wafer and freeze-drying it overnight. AFM ([**1**] = 0.1 mM) images of the diluted solution of the metallo(ge)l of **1** at different position and magnifications respectively.
8. Figure S6: DLS studies of the diluted solution of the metallo(ge)l ([**1**] = 2 mM) and reduction in the size of the NMOPs after addition of one and three equiv. of pyridine with respect to the one equiv. of compound **1** to the solution respectively. DLS studies of the solution of compound **1** ([**1**] = 2 mM) in water under identical condition.
9. Figure S7: Concentration-dependent UV-Vis absorption spectra of the metallo(ge)l. EPR spectra of the diluted solution of the metallo(ge)l from the 1:1 acetonitrile-toluene mixture; [**1**] = 1 mM.
10. Figure S8: Oscillatory frequency sweep experiments of the metallo(ge)l of **1** at three different concentrations.
11. Figure S9: Injectability of the hydrogel has been demonstrated by writing different alphabetical letters on top of a glass plate.

Physical Measurements and Instrumentation.

Gelation Studies. The detail procedure for hydrogelation was discussed in the main paper. The formation of the gel was confirmed using tube inversion method. If a gel was formed, it was evaluated quantitatively by determining the critical gelator concentration (CGC), which is the minimum amount of gelator required to immobilize 1 mL of water. Gelation test including evaluation of CGC was carried out in test tubes with capacity: 10x75 mm.

FT-IR Spectroscopy. Solutions of the compounds/mixtures were drop-cast on the CaF₂ cell and dried under vacuum and the spectra were recorded in Perkin Elmer Spectrum BX FT-IR system.

UV-Vis absorption and Fluorescence Spectroscopy. The UV-Vis and fluorescence spectra of solutions were recorded on Shimadzu model 2100 spectrophotometer and Hitachi F-4500 spectrofluorimeter respectively, both equipped with a temperature controller bath.

EPR Spectroscopy. The X-band (9.44GHz) EPR spectrum of the 1:1 acetonitrile-toluene solution of the metallogel ([1] = 1 mM) was obtained at 77 K on a Bruker A300 spectrometer, equipped with an ER 4141VT cryostat with 100 kHz field modulation. (Modulation amplitude = 5 G and Microwave power = 22.32 mW).

Scanning Electron Microscopy (SEM). The gels or diluted solutions of the aggregates were carefully drop-casted onto the silicon wafer and were allowed to freeze-dry overnight. The samples were then coated with gold vapour and analyzed on a Quanta 200 SEM operated at 10-15 kV.

Atomic Force Microscopy (AFM). Solutions of the aggregates were drop-casted on mica strips and then carefully freeze-dried. Each of the samples were analyzed using JPK 00901 instrument and Nano-Wizard software: Tapping mode, 10 nm tip radius, silicon tip, 292 KHz resonant frequency, 0.7-1 Hz scan speed, 256x256 and 512x512-pixels.

Dynamic Light Scattering (DLS). DLS measurements were performed at room temperature using a Malvern Zetasizer NanoZS particle sizer (Malvern Instruments Inc., MA) instrument. Diluted solutions of the metallogel were examined under dust-free conditions. Average hydrodynamic diameters (D_h) reported were obtained from Gaussian analysis of the intensity-weighted particle size distributions.

Rheological Studies. For rheology experiment of the gels, an Anton Paar 100 rheometer with a cone and plate geometry (CP 25-2) having an adjustable peltier temperature controlling system was used. All the measurements were done fixing the gap distance between the cone and the plate at 0.05 mm. The gels were scooped on the plate of the rheometer. An oscillatory strain amplitude sweep experiment was performed at a constant oscillation frequency of 1 Hz for the applied strain range 0.001-300 % at 20 °C. The software US-200 converted the torque measurements into either G' (the storage modulus) and G'' (the loss modulus) and represent G' and G'' with either strain or shear stress. Oscillatory frequency sweep experiments were performed in the linear viscoelastic region (strain 0.01%) to ensure that calculated parameters correspond to an intact network structures.

X-ray Diffraction. Gels were scooped onto glass slide and kept under reduced pressure for 24 h for the corresponding XRD measurement. These samples were analyzed using a Bruker D8 Advance instrument (θ , 2 θ geometry with Scintillation Detectors). The X-ray beam generated with rotating Cu anode at the wavelength of KR beam at 1.5418 Å was directed toward the film edge and scanning was done up to a 2 θ value of 30°. Data were analyzed and interpreted using the Bragg equation.

Energy Minimization. Energy minimization of the 1/Cu²⁺ complex was performed using B3LYP/6-31G* level of computations.

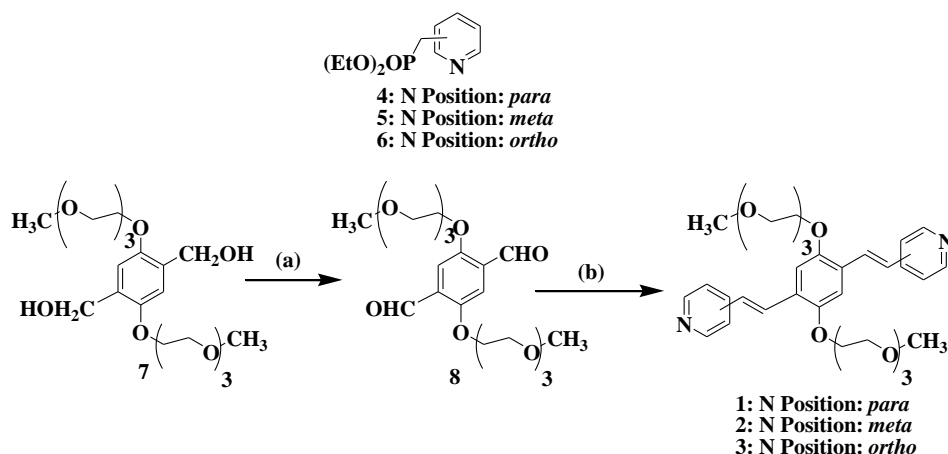
Electroluminescence (EL) Studies. ITO coated glass substrates were etched selectively using diluted aqua regia to form the bottom electrodes. The substrates were cleaned using acetone, 1-propanol and distilled water. Following that, the films of gels were coated on patterned ITO substrates using spin coating process. Au top electrode was deposited by thermal evaporation with a base pressure of 8.5x10⁻⁶ mbar using a shadow mask of area 0.2x0.2 cm². The voltage varying between +/- 0 to 16V has been applied across the electrodes for the EL measurements using a monochromator and a PMT detector.

Elemental Analysis of the Metallogel. A reaction of the compound 1 and the CuCl₂.2H₂O at a 1:1 molar ratio in CH₃CN in diluted condition has been carried out. This resulted in the formation of precipitate almost

instantaneously. The mixture was then centrifuged. TLC of the supernatant showed almost complete disappearance of the starting compound **1**. The residue obtained after centrifugation, on the other hand, was re-suspended in minimum amount of CH₃CN and the same procedure is followed to remove any unreacted starting materials. Finally, the precipitate was dried under vacuum for 24 h and subjected to elemental analysis with the resultant solid. Elemental analysis of the resultant solid afforded the following data: C, 52.31; H, 6.21; N, 3.73. This data is in agreement with the molecular formula or repetitive unit of the metallogel as Cu(Py)₂Cl₂(H₂O)₂ (C, 52.41; H, 6.21; N, 3.6; Py denotes the end pyridyl units of the compound **1**).

2a. Materials and Methods: All chemicals, solvents and silica gel for TLC were obtained from well-known commercial sources and were used without further purification, as appropriate. Solvents were distilled and dried by standard procedure before use. ¹H-NMR and ¹³C-NMR spectra were recorded in Bruker-400 Advance NMR spectrometer. Chemical shifts were reported in ppm downfield from the internal standard tetramethylsilane (TMS). Mass spectrometry of individual compounds was performed using a MicroMass ESI-TOF MS instrument. Elemental analysis was recorded in Thermo Finnigan EA FLASH 1112 SERIES.

2b. General Synthetic Scheme: The synthesis of the bis-alcohol (**7**)^(S1) and n-[(Diethylphosphono)methyl]pyridine^(S2) (**4**, **5** and **6**) were carried out according to reported procedures in literature. Scheme showing routes to **1**, **2** and **3** was shown below.



Reagents, conditions and yields: (a) PCC, dry DCM, rt, 2h, 90.8%; (b) **4**, **5** or **6**, ^tBuOK, dry THF, rt, 6-8 min, 98.3% for **1**; 95% for **2** and 93% for **3** respectively.

2c. Synthesis and Characterization:

Bis-aldehyde (8): To a solution of **7** (2 g, 4.3 mmol) in 50 ml of dry DCM, PCC (3.73 g, 17.3 mmol) was added at a time. The mixture was stirred for 2 h at room temperature. After completion of the reaction small amount of silica gel was added to the round bottom flask and adsorbed by a low pressure vacuum pump. It was then packed in an open column (SiO₂) and the product was eluted with 3 % MeOH/CHCl₃ solution. 1.8 g of **8** was isolated as a light yellow oil: yield 90.8%; ¹H NMR (400 MHz, CDCl₃) δ 3.37 (s, 6H); 3.54-3.56 (m, 4H), 3.64-3.68 (m, 8H), 3.71-3.74 (m, 4H), 3.88-3.91 (m, 4H), 4.27 (t, J = 4.8 Hz, 4H), 7.46 (s, 2H), 10.52 (s, 2H); ¹³C NMR (400 MHz, CDCl₃) δ 58.9, 68.8, 69.4, 70.5, 70.6, 70.8, 71.8, 112.1, 129.4, 155.1, 189.2; HRMS *m/z* calcd for C₂₂H₃₄O₁₀ (M + Na)⁺ 481.22, found 481.2050.

Synthesis of ligand 1: To a solution of the bis-aldehyde (**8**) (1.23 g, 2.68 mmol) and 4-[(diethylphosphono)methyl]-pyridine (**4**) (1.23 g, 5.37 mmol) in dry THF (20 ml), ^tBuOK (1.2 g, 10.72 mmol) was added and the solution was stirred at room temperature for 6 min. After completion of the reaction, a few drops of water were added to the reaction mixture. Solvent was evaporated under high vacuum and the product was purified by flash column chromatography (SiO₂) using 3.5% MeOH/CHCl₃ solution. **1** was isolated as a wax like solid in almost quantitative yield: yield 98.3 %; IR (Neat, cm⁻¹) 2925, 2877, 1596, 1495, 1416, 1351, 1202, 1109; ¹H NMR (400 MHz, CDCl₃) δ 3.35 (s, 6H), 3.51-3.54 (m, 4H), 3.64-3.66 (m, 4H), 3.69-3.72 (m, 4H), 3.78-3.80 (m, 4H), 3.93-3.95 (m, 4H), 4.24-4.26 (m, 4H), 7.06 (d, J = 16.4 Hz, 2H), 7.18 (s, 2H), 7.39 (d, J

= 5.6 Hz, 4H), 7.65 (d, J = 16.4 Hz, 2H), 8.57 (d, J = 5.6 Hz, 4H); ^{13}C NMR (400 MHz, CDCl_3) δ 58.98, 69.16, 69.80, 70.55, 70.66, 70.83, 71.86, 111.62, 120.89, 126.87, 127.1, 127.64, 145.03, 150.08, 151.41; HRMS m/z calcd for $\text{C}_{34}\text{H}_{44}\text{N}_2\text{O}_8$ ($\text{M} + \text{H}$) $^+$ 609.31, found 609.3204; Elemental analysis: calcd for $\text{C}_{34}\text{H}_{44}\text{N}_2\text{O}_8 \cdot \text{H}_2\text{O}$: C, 65.16; H, 7.4; N, 4.47; Found: C, 65.33; H, 7.31; N, 4.59.

Synthesis of ligand 2: To a solution of bis-aldehyde (**8**) (0.12 g, 0.26 mmol) and 3-[(diethylphosphono)methyl]-pyridine (**5**) (0.12 g, 0.52 mmol) in dry THF (8 ml), $^t\text{BuOK}$ (0.12 g, 1.05 mmol) was added and the solution was stirred at room temperature for 6-8 min. After completion of the reaction, a few drops of water were added to the reaction mixture. Solvent was evaporated using high vacuum and the product was purified by flash column chromatography (SiO_2) using 3% $\text{MeOH}/\text{CHCl}_3$ solution. **2** was isolated as a wax like solid: yield 95 %; IR (Neat, cm^{-1}) 2918, 2876, 1635, 1442, 1259, 1205, 1110, 1060, 1019; ^1H NMR (400 MHz, CDCl_3) δ 3.35 (s, 6H), 3.51-3.54 (m, 4H), 3.63-3.66 (m, 4H), 3.69-3.71 (m, 4H), 3.78-3.8 (4H), 3.93-3.95 (m, 4H), 4.24-4.26 (m, 4H), 7.1 (d, J = 16.4 Hz, 2H), 7.18 (s, 2H), 7.28 (2H), 7.51 (d, J = 16.4 Hz, 2H), 7.87 (d, J = 8 Hz, 4H), 8.47 (d, J = 4 Hz, 2H), 8.73 (broad singlet, 2H); ^{13}C NMR (400 MHz, CDCl_3) δ 58.95, 69.22, 69.86, 70.5, 70.71, 70.85, 71.87, 111.42, 123.52, 125.34, 125.43, 125.55, 127.12, 132.67, 133.47, 148.36, 148.59, 151.14; HRMS m/z calcd for $\text{C}_{34}\text{H}_{44}\text{N}_2\text{O}_8$ ($\text{M} + \text{H}$) $^+$ 609.31, found 609.3176; Elemental analysis: calcd for $\text{C}_{34}\text{H}_{44}\text{N}_2\text{O}_8 \cdot \text{H}_2\text{O}$: C, 65.16; H, 7.4; N, 4.47; Found: C, 65.41; H, 7.51; N, 4.39.

Synthesis of ligand 3: To a solution of bis-aldehyde (**8**) (0.1 g, 0.22 mmol) and 2-[(diethylphosphono)methyl]-pyridine (**6**) (0.1 g, 0.44 mmol) in dry THF (20 ml), $^t\text{BuOK}$ (0.1 g, 0.87 mmol) was added and the solution was stirred at room temperature for 8 min. After completion of the reaction, a few drops of water were added to the reaction mixture. Solvent was evaporated using high vacuum and the product was purified by flash column chromatography (SiO_2) using 2-3% $\text{MeOH}/\text{CHCl}_3$ solution. **3** was isolated as a wax like solid: yield 93 %; IR (Neat, cm^{-1}) 2922, 2876, 1584, 1471, 1435, 1246, 1212, 1109, 1025; ^1H NMR (400 MHz, CDCl_3) δ 3.34 (s, 6H), 3.5-3.53 (m, 4H), 3.64-3.66 (m, 4H), 3.69-3.71 (m, 4H), 3.78-3.8 (m, 4H), 3.92-3.95 (m, 4H), 4.22-4.24 (m, 4H), 7.21 (s, 2H), 7.25 (d, J = 16.4 Hz, 2H), 7.27 (2H), 7.46 (d, J = 8 Hz, 2H), 7.65-7.68 (m, 2H), 7.86 (d, J = 16.4 Hz, 2H), 8.58 (d, J = 4 Hz, 2H); ^{13}C NMR (400 MHz, CDCl_3) δ 58.94, 68.98, 69.80, 70.49, 70.65, 70.87, 71.87, 111.91, 121.52, 121.83, 126.84, 127.12, 129.21, 136.38, 149.54, 151.41, 156.56; HRMS m/z calcd for $\text{C}_{34}\text{H}_{44}\text{N}_2\text{O}_8$ ($\text{M} + \text{H}$) $^+$ 609.31, found 609.3175; Elemental analysis: calcd for $\text{C}_{34}\text{H}_{44}\text{N}_2\text{O}_8 \cdot \text{H}_2\text{O}$: C, 65.16; H, 7.4; N, 4.47; Found: C, 65.35; H, 7.48; N, 4.61.

References.

- (S1) G. Fabbrini, R. Ricc , E. Menna, M. Maggini, V. Amendola, M. Garbin, M. Villano, M. Meneghetti, *Phys. Chem. Chem. Phys.* 2007, **9**, 616.
- (S2) (a) A. J. Hutchison, M. Williams, C. Angst, R. de Jesus, L. Blanchard, R. H. Jackson, E. J. Wilusz, D. E. Murphy, P. S. Bernard, J. Schneider, T. Campbell, W. Guida and M. A. Sills, *J. Med. Chem.* 1989, **32**, 2171; (b) R. Laufer, B. Forrest, S. Li, Y. Liu, P. Sampson, L. Edwards, Y. Lang, D. E. Awrey, G. Mao, O. Plotnikova, G. Leung, R. Hodgson, I. Beletskaya, J. M. Mason, X. Luo, X. Wei, Y. Yao, M. Feher, F. Ban, R. Kiarash, E. Green, T. W. Mak, G. Pan and H. W. Pauls, *Journal of Med. Chem.* 2013, **56**, 6069; (c) Y. Okamoto, I. Kokubo and S. Takamuku, *Bull. Chem. Soc. Jpn.* 1990, **63**, 2438.

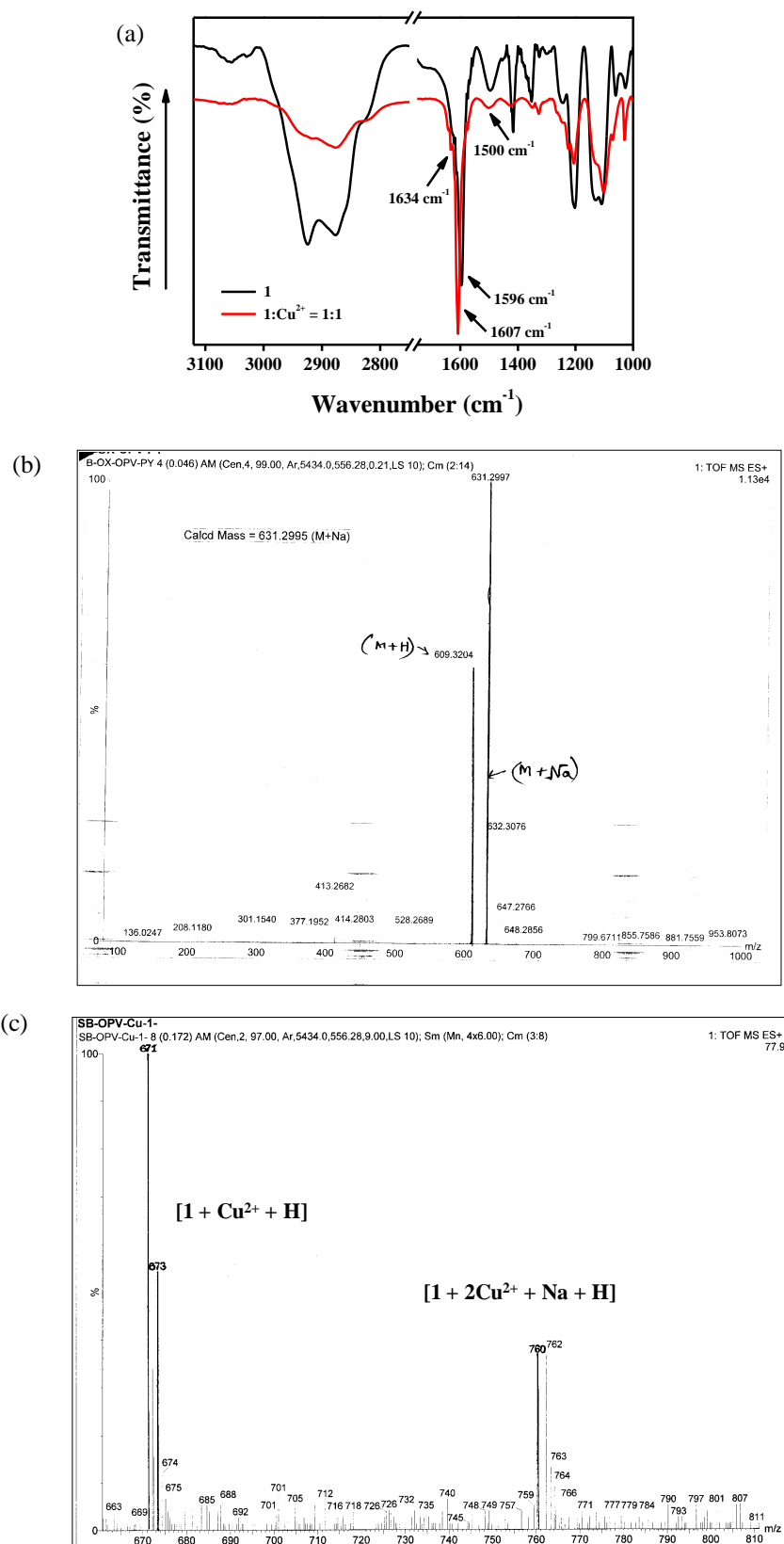


Figure S1. (a) FT-IR spectra of ligand **1** and **1**:Cu²⁺ complex. (b,c) ESI-MS of **1** and **1**:Cu²⁺ complex respectively.

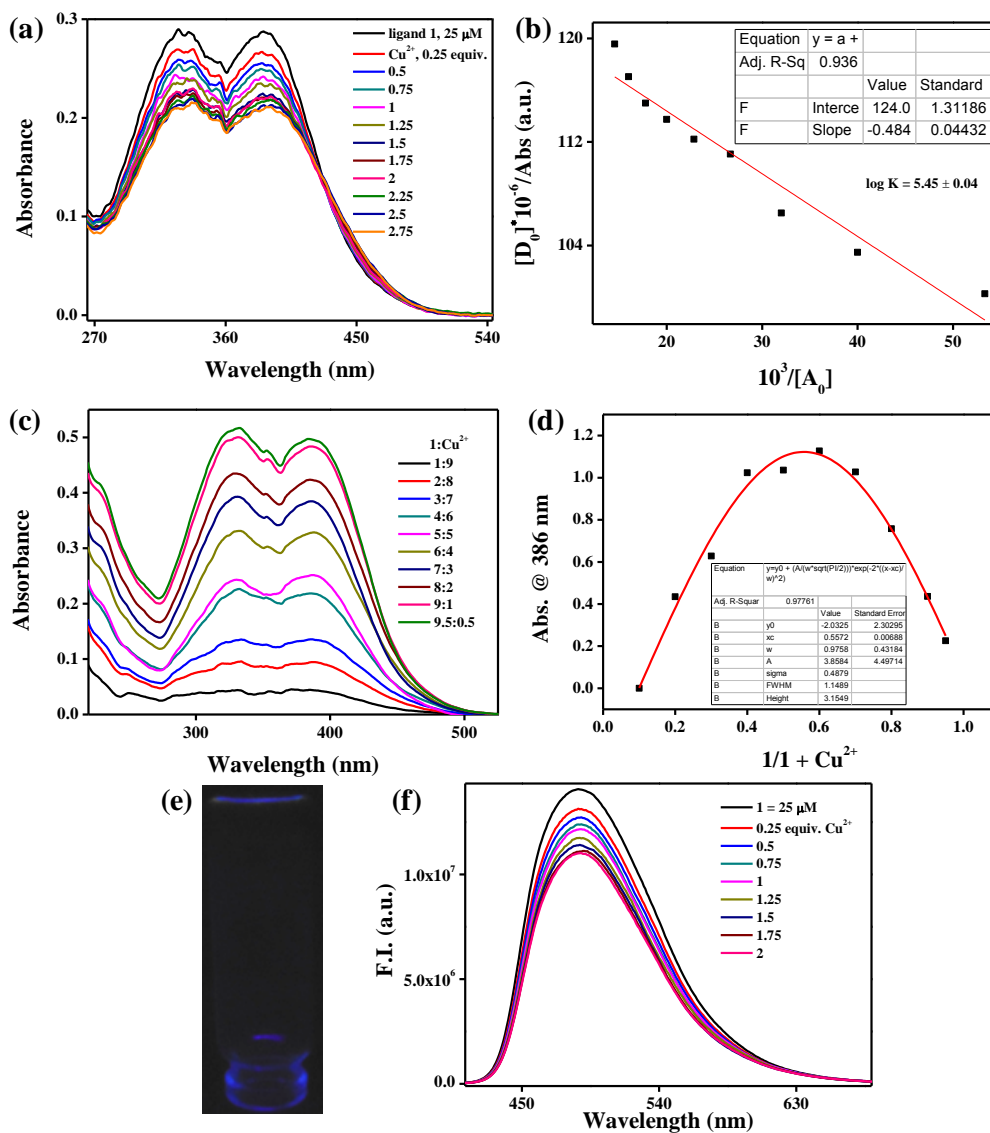


Figure S2. (a) Titration of ligand **1** with increasing amount of Cu^{2+} in water under UV-Vis spectroscopy ($[\mathbf{1}] = 25 \mu\text{M}$) and (b) determination of binding constant of the $1/\text{Cu}^{2+}$ complex. (c) UV-Vis spectroscopy of the solution of $1/\text{Cu}^{2+}$ in various molar ratios at a fixed total concentration of 50 μM . (d) Job's plot of **1** with Cu^{2+} in water. (e) Digital image of the metallogel of **1** under illumination at 365 nm. (f) Titration of the suspension of the ligand **1** (25 μM) in water with increasing proportion of Cu^{2+} .

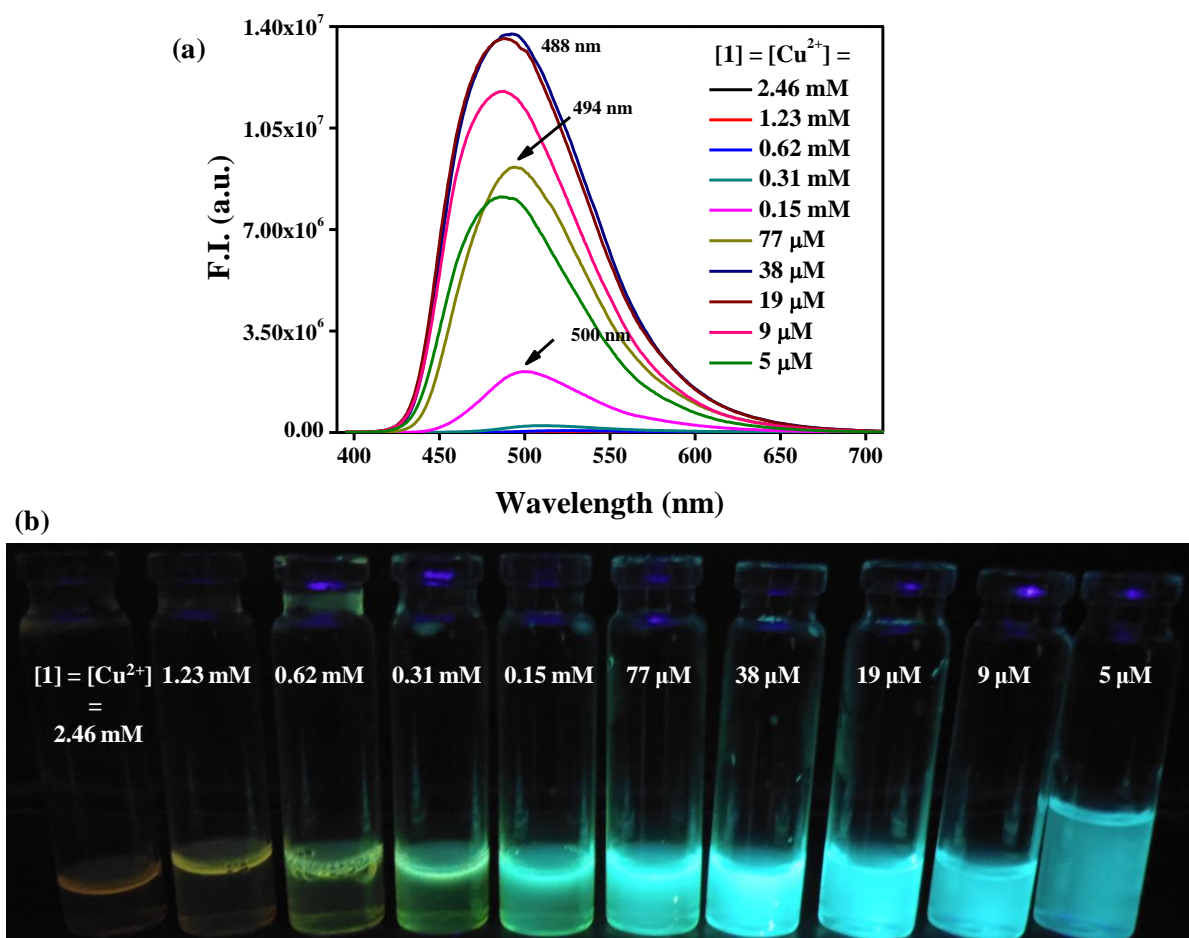


Figure S3. (a,b) Concentration dependent emission spectra of the metallogel and the corresponding photographs of the solutions under UV-light (365 nm) respectively.

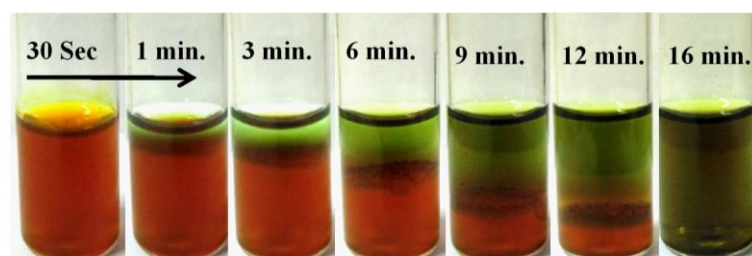


Figure S4. Demonstration of the gradual abolition of the metallogel of **1**, when a few drops of conc. NH_4OH solution were added to the top of the preformed gel.

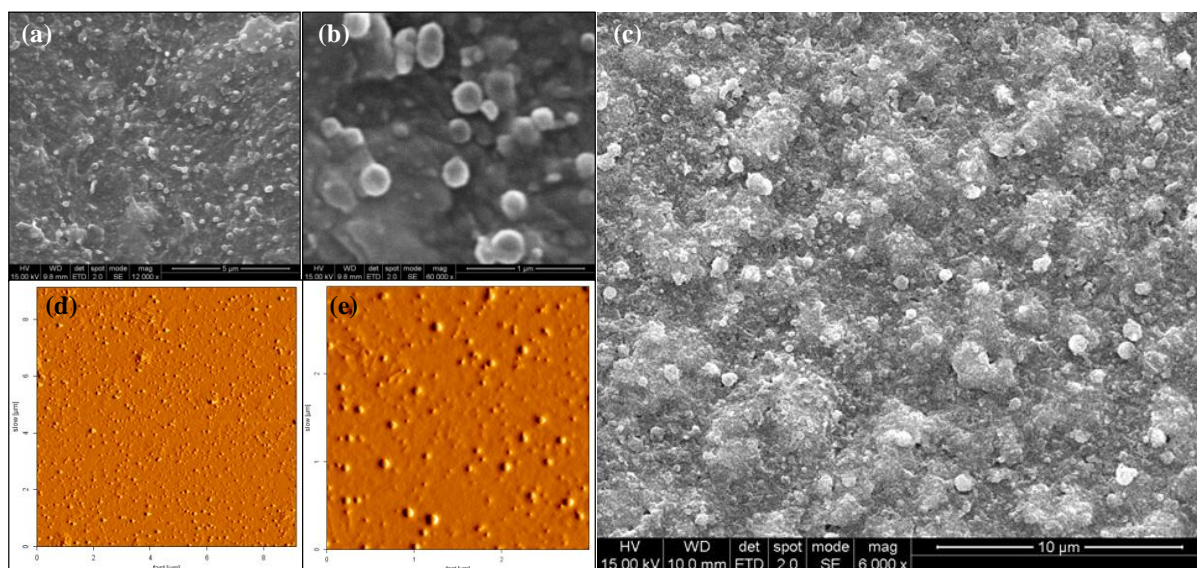


Figure S5. (a,b) SEM ($[1] = 0.3 \text{ mM}$) images of the diluted solution of the metallogel of **1** at different position and magnifications respectively. (c) SEM ($[1] = 8 \text{ mM}$) image of the metallogel of **1** obtain after drop-casting of the metallogel directly onto the silicon wafer and freeze-drying it overnight. (d,e) AFM ($[1] = 0.1 \text{ mM}$) images of the diluted solution of the metallogel of **1** at different position and magnifications respectively.

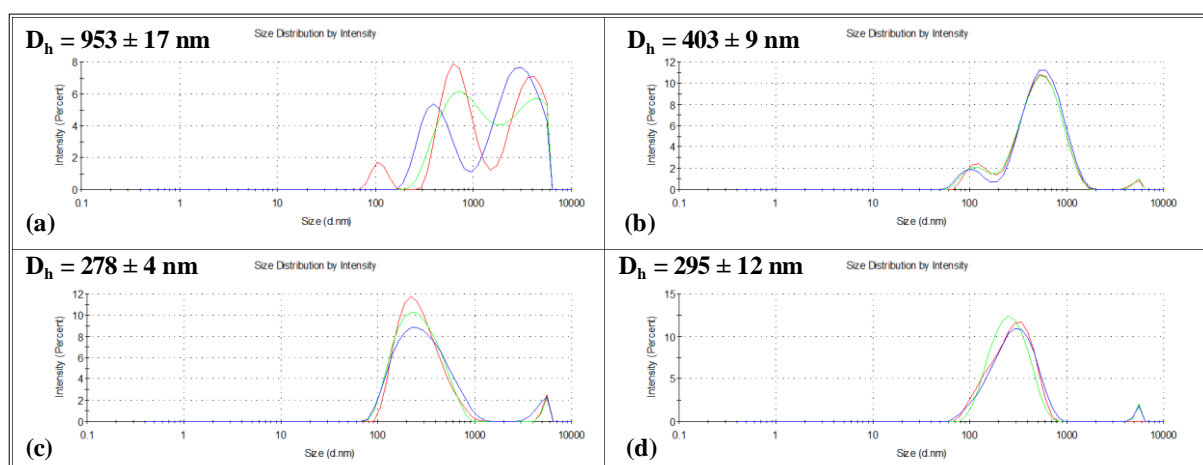


Figure S6. (a) DLS studies of the diluted solution of the metallogel ($[1] = 2 \text{ mM}$) and reduction in the size of the NMOPs after addition of (b) one and (c) three equiv. of pyridine with respect to the one equiv. of compound **1** to the solution respectively. (d) DLS studies of the solution of compound **1** ($[1] = 2 \text{ mM}$) in water under identical condition.

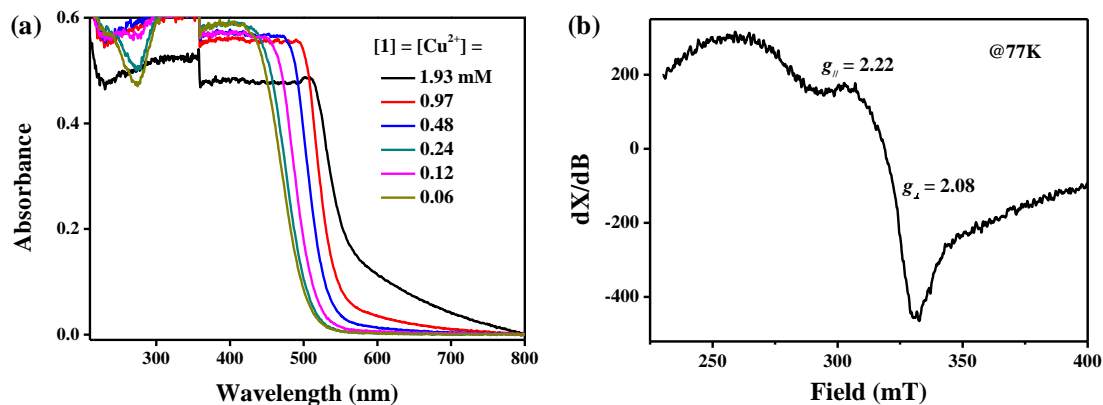


Figure S7. (a) Concentration-dependent UV-Vis absorption spectra of the metallogel. (b) EPR spectra of the diluted solution of the metallogel from the 1:1 acetonitrile-toluene mixture; $[1] = 1 \text{ mM}$.

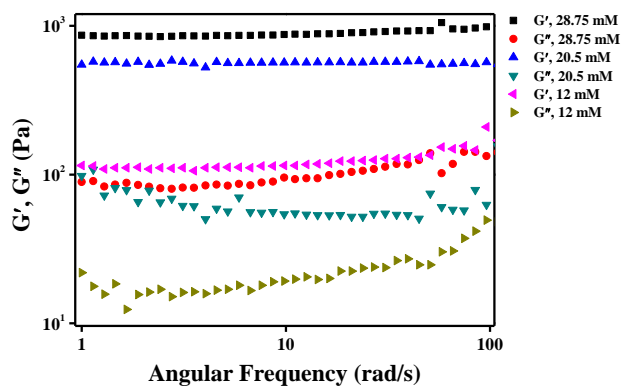


Figure S8. Oscillatory frequency sweep experiments of the metallogel of **1** at three different concentrations.



Figure S9. Injectability of the hydrogel has been demonstrated by writing different alphabetical letters on top of a glass plate.